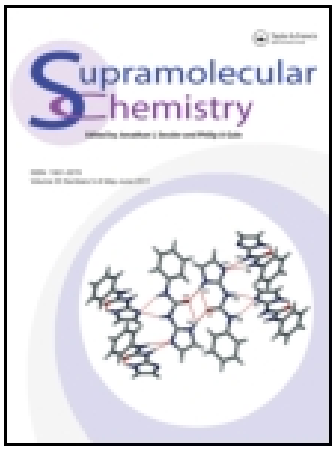

Supramolecular Chemistry
Publication details, including instructions for authors and subscription information:
http://www.tandfonline.com/loi/gsch20

Chromogenic amides of pyridine-2,6-dicarboxylic acid as anion receptors

Ewa Wagner-Wysiecka [a] & Jarosław Chojnacki [b]

[a] Department of Chemical Technology , Chemical Faculty, Gdansk University of Technology , Narutowicza11/12, 80-233 , Gdansk , Poland

[b] Department of Inorganic Chemistry , Chemical Faculty, Gdansk University of Technology , Narutowicza11/12, 80-233 , Gdansk , Poland

Published online: 20 Jun 2012.

To cite this article: Ewa Wagner-Wysiecka & Jarosław Chojnacki (2012) Chromogenic amides of pyridine-2,6-dicarboxylic acid as anion receptors, Supramolecular Chemistry, 24:9, 684-695, DOI: 10.1080/10610278.2012.695789

To link to this article: http://dx.doi.org/10.1080/10610278.2012.695789

Supramolecular Chemistry
Vol. 24, No. 9, September 2012, 684–695

Chromogenic amides of pyridine-2,6-dicarboxylic acid as anion receptors

Ewa Wagner-Wysiecka[a]* and Jarosław Chojnacki[b]

[a]*Department of Chemical Technology, Chemical Faculty, Gdansk University of Technology, Narutowicza11/12, 80-233 Gdansk, Poland;*
[b]*Department of Inorganic Chemistry, Chemical Faculty, Gdansk University of Technology, Narutowicza11/12, 80-233 Gdansk, Poland*

(*Received 19 January 2012; final version received 9 May 2012*)

The synthesis of simple, chromogenic pyridine-2,6-dicarboxylic acid amides, derivatives of isomeric nitroanilines and aminonitrophenols, and their ion binding properties are described. The ligands' response to ionic species was examined by naked eye and was studied with the use of UV–vis spectroscopy in DMSO and its mixture with water. The effect of the localisation and the type of the substituents in aromatic rings were discussed. ^{1}H NMR experiments were carried out to probe the mechanism of anion recognition, i.e. complexation *via* hydrogen bond formation versus ligand deprotonation. A selective response of *N*,*N*′-bis(2-hydroxy-4-nitrophenyl)pyridine-2,6-dicarboxamide (**L5**) towards dihydrogen phosphate was found in both DMSO and DMSO–water (95:5) solvent mixture. The structure of *N*,*N*′-bis(2-hydroxy-5-nitrophenyl)pyridine-2,6-dicarboxamide (**L4**) was confirmed by X-ray crystallography.

Keywords: chromogenic amides; anion recognition; hydrogen bonds; UV–vis spectroscopy; NMR spectroscopy

1. Introduction

After several decades, when very broad interest in supramolecular chemistry was connected with metal cation complexation, the present time seems to be a 'golden age' for anion coordination chemistry. There are a number of reasons for still growing interest in anion recognition. Anions play an important role in many biological processes, e.g. carrying genetic information (polyanionic DNA); a majority of enzyme substrates and cofactors are anionic. There is also a dark side of ubiquitous anions. Some may disadvantageously influence the environment and human health or even life. For example, phosphates and nitrates as fertilisers cause eutrophication of natural waters (*1*); metabolites of nitrates are known to be carcinogenic for many years (*2*). Fluorides widely used in toothpastes may also cause serious diseases (*3a*, *b*). Although the nature is the most perfect synthetic and self-monitoring laboratory, the design and synthesis of artificial anion receptors allows us to mimic natural systems and learn about mechanisms of biochemical processes, and also gives a useful analytical tool for anion detection and determination.

Anionic species are challenging targets for recognition studies because of several features, such as their wide range of sizes and shapes, diverse hydrophobicity, pH-dependent charge, etc. There are many reasons why the design of sufficiently selective anion receptors is not always easy. This topic and many other important aspects related to anion complexation by different types of receptors have been exhaustively discussed in comprehensive reviews (*4a–i*). The anion–ligand interaction may be of electrostatic nature, formation of hydrogen bonds, binding anions by electron-deficient Lewis acidic centres, anion–π, π–π interactions or of sum of all these (or part of them) relating to both the host and the guest as well as their surroundings.

One of the most popular constituents of building blocks for anion receptors are groups that are able to form hydrogen bond(s) (*5*). Such interactions utilising N—H hydrogen donor groups are found in many types of artificial anion receptors as calyx[*n*]pyrroles (*6*), urea and thiourea derivatives (*7*), sulfonamides (*8*) and amides (*9a*, *b*). A series of amide anion receptors, containing among others 2,6-diamidopyridine and 1,3-diamidobenzene as building blocks, have been described by Jurczak and co-workers (*10a–d*). Pyridine, pyrrole, imidazole or more sophisticated heterocyclic residues are often introduced into an anion receptor forming primary or supplementary parts of the ligand bearing hydrogen bond acceptor(s) and/or donor(s) (*11*, *12*). Besides N—H protons, also other centres such as O—H (*13a–c*) or C—H (*14a–c*) may be involved in hydrogen bond formation. Such systems, i.e. utilising OH and CONH groups, occur in natural anion binding sites of peptides (*15a*, *b*).

Data about anion–receptor interaction may be rapidly acquired by enriching the ligand structure with chromophore residue(s), resulting in the formation of chromogenic molecule. Due to cooperation of receptor and

*Corresponding author. Email: ewa.wagner-wysiecka@pg.gda.pl

ISSN 1061-0278 print/ISSN 1029-0478 online

http://dx.doi.org/10.1080/10610278.2012.695789
http://www.tandfonline.com

chromophoric parts, ion binding could be observed with a 'naked eye'. It also enables simple tracing of complexation process using UV–vis spectroscopy. A considerable number of publications in recent years concern chromogenic anion receptors, suggesting a major interest in this area. Different types of chromogenic anion receptors have been described in review articles by Suksai and Tuntulani (*4e*, *16*). Another review article by Martinez-Máñez and Sancenón (*17*) has presented both chromogenic and fluorogenic anion receptors showing different design principles for anion sensing. Colorimetric anion sensors differ from each other not only by the arrangement of receptor site, but also by types of chromogenic residues that are responsible for transduction of recognition information into optical signal. Several of these compounds may act as both colorimetric and fluorescent anion chemosensors. For examples of different types of anion receptors, see Refs (*18–26*).

In this paper, the synthesis of simple chromogenic pyridine-2,6-dicarboxylic acid (dipicolinic acid) amides **L1**–**L5** (Figure 1) is presented. These receptors were investigated as colorimetric and 'naked eye' sensors for ionic species, mainly anions, in DMSO, an aprotic solvent, and its mixture with water. The effect of the localisation and the type of the benzene ring substituents are discussed, and the possible mechanism of anion recognition is proposed.

2. Results and discussion

2.1 Synthesis and characterisation of ligands L1–L5

Ligands **L1**–**L5** were prepared using a facile reaction of commercially available 2,6-pyridine dicarboxylic acid chloride with isomeric nitroanilines or aminonitrophenols in DMF and in the presence of triethylamine. The general synthetic route is shown in Figure 1.

Pure compounds were obtained after crystallisation from methanol; in most cases, the yield was high (about 90%). Their structures were confirmed by high-resolution mass spectra and ^{1}H NMR, ^{13}C NMR and FTIR spectroscopy. Among all presented ligands, to the best our knowledge – on the basis of Chemical Abstracts, only **L3** has been reported in literature until now. The reported method, where acetonitrile (*25*) was used as a solvent, gives a significantly lower yield (52% for **L3**) of the desired compounds.

2.2 Complexation studies

Compounds presented in Figure 1, until now, were not examined as chromogenic anion sensors, except **L3**, for which colorimetric anion-sensing properties and mechanism of anion recognition were studied (*25*, *26*). Three pseudo-polymorphs of **L3** were characterised by X-ray crystallography (*27*). It has also been reported (*28*) that **L3** can efficiently bind to ruthenium(II).

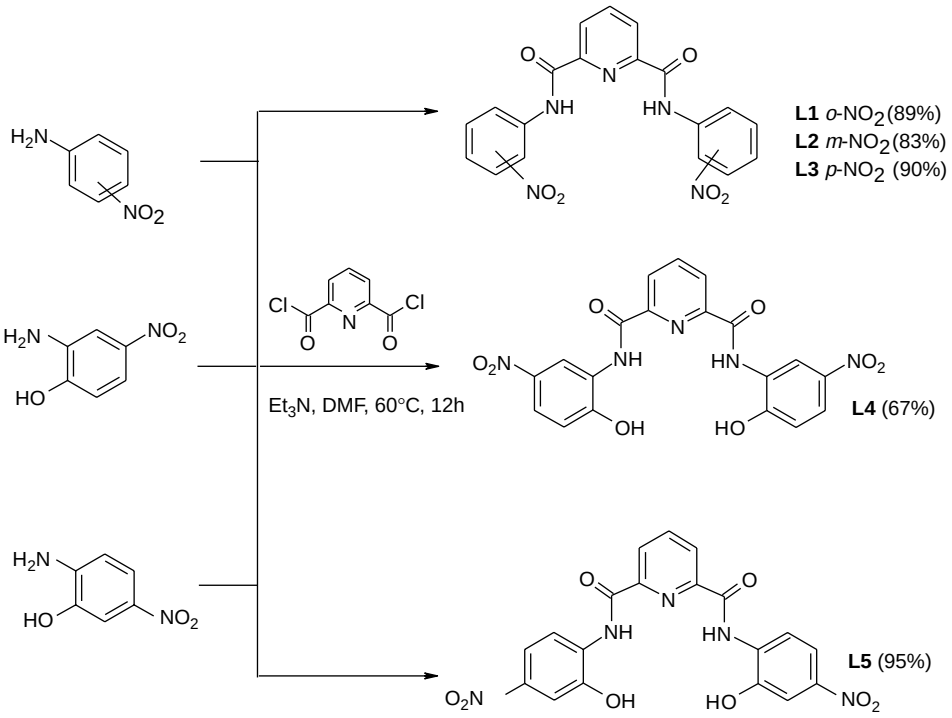

Figure 1. Synthetic route leading to chromogenic diamides **L1**–**L5**.

Here, we report metal cation and anion binding studies for ligands **L1**–**L5**. Complexation investigations were carried out using UV–vis spectrophotometry in DMSO as a solvent. The studied metal cations were alkali (Li^+, Na^+, K^+), alkaline earth (Mg^{2+}, Ca^{2+}, Sr^{2+}, Ba^{2+}) and heavy divalent metal cations (Co^{2+}, Ni^{2+}, Zn^{2+}, Cu^{2+}, Pb^{2+}) used in the form of perchlorates. No significant changes in absorption spectra, recorded in DMSO, were found in the presence of all studied metal cations. It means that these cations used as counterions should not affect anion complexation, although in the studies presented only tetra-*n*-butylammonium (TBA) salts were used for anion complexation. To study the anion–ligand interactions, anions of different sizes and shapes were chosen: spherical (halides), linear (thiocyanate), V-shaped (simple carboxylates: acetate, benzoate, tosylate), trigonal-planar (nitrate) and tetrahedral (dihydrogen phosphate, hydrogen sulphate, perchlorate). Anion complexation was examined in pure DMSO and mixed DMSO–water (95:5, v/v) solvent system.

As anion recognition *via* hydrogen bonding is not always easy to differentiate from deprotonation of N—H and/or O—H residues, experiments with tetra-*n*-butylammonium hydroxide (TBAOH) were also carried out. Preliminary studies of the complexation mechanism were performed using ^{1}H NMR spectroscopy.

For derivatives of isomeric nitroanilines **L1**–**L3**, spectral and colour changes were observed in DMSO only in the presence of fluorides among the above listed salts. Halide anions, other than fluorides, do not cause colour change, even if used in large excess (saturated solutions). The pale yellow (**L1** and **L3**) or almost colourless (**L2**) solution in DMSO turned intensively yellow after fluoride addition (50 equiv.) with the most pronounced changes for the *para*-substituted nitroaniline derivative (**L3**) (Figure 2). The smaller amounts of tetra-*n*-butylammonium fluoride (TBAF) (1 equiv.) cause a visible, but less significant colour change for **L3**. For better visualisation of colour changes of **L1**–**L3** in the presence of fluorides, a large excess is more favourable. Almost the same trends were observed upon gradual addition of TBAOH. The observable colour changes for **L3** could be easily explained by the electron-withdrawing effect of the nitro group in relation to the *para* amide moiety, strongly influencing acidity of N—H protons.

Figure 2. Colour changes of **L1**–**L3** (8.1×10^{-5} M) observed upon addition of 50-fold excess of TBAF and TBAOH.

The comparison of the spectral changes upon titration of **L1**–**L3** with TBAF and TBAOH in DMSO is shown in Figure 3(a)–(d).

The colour changes increase in the order **L3** > **L1** > **L2**. It is in agreement with the observed colour changes in the presence of an excess of fluorides. From the titration course it may be concluded for all cases that more than one equilibrium exists under titration conditions. The appearance of a new band, of a relatively large bathochromic shift and not a sharp isosbestic point for **L3** and **L1**, as well as the trend of changes for **L2** may suggest that two-step deprotonation of the ligands is responsible for colour changes rather than anion complexation *via* hydrogen bond formation. The other possibility is the ligand–anion interaction *via* hydrogen bond formation at low TBAF concentration and deprotonation of the ligand in the presence of an excess of basic fluorides. The most probable deprotonation process is supported by the fact that almost identical spectral changes for the investigated ligands were observed when titrated with TBAOH and TBAF (Figure 3(d)). Relatively low concentrations of the reactants, which are required for typical UV–vis titrations, indicate that deprotonation is more favoured than it is at higher concentration levels (both the ligand and the respective salt), where the deprotonation degree is smaller (*13b*, *29*). Thus, further studies on the nature of ligand–anion interactions were carried out by analysing the ^{1}H NMR titration of **L3** (4.62×10^{-3} M) with TBAF, i.e. at a concentration level of about two orders of magnitude higher than that for UV–vis spectroscopic experiments. Spectra were registered in DMSO-d_6. As a model compound, **L3** was chosen, due to the most significant colour and spectral changes. Figure 4(a) displays ^{1}H NMR spectra (range 8–17 ppm) of **L3** titration with fluoride salt.

The N—H signal at 11.44 ppm broadens and dramatically shifts downfield upon addition of fluoride ions. In the presence of 1 equiv. of TBAF, the N—H signal appeared at 15.6 ppm as a broad singlet, suggesting existence of an intramolecular hydrogen bonding between fluoride anion and ligand, in which N—H amide protons are involved. Moreover, aromatic proton signals of the neighboring C—H appearing as a doublet at 8.47 ppm for free ligand are also shifted downfield (8.55 ppm). Upon addition of 1.2 equiv. of fluorides the N—H signal appeared at 16.1 ppm as a distorted singlet and, finally, in the presence of ~2 equiv. of fluorides, this signal was observed at 16.3 ppm (t, $J = 119$ Hz) and did not shift (upon further increase of titrant concentration). This signal may be attributed to HF_2^- formation under measurement conditions. Considering that both amide NH moieties in U-shaped, 2,6-pyridinediamides preferably exist in a *syn*–*syn* conformation (*30a*–*c*) and pyridine nitrogen is involved in formation of intramolecular hydrogen bond, the mechanism of fluoride binding proposed here is shown in Scheme 1. In the

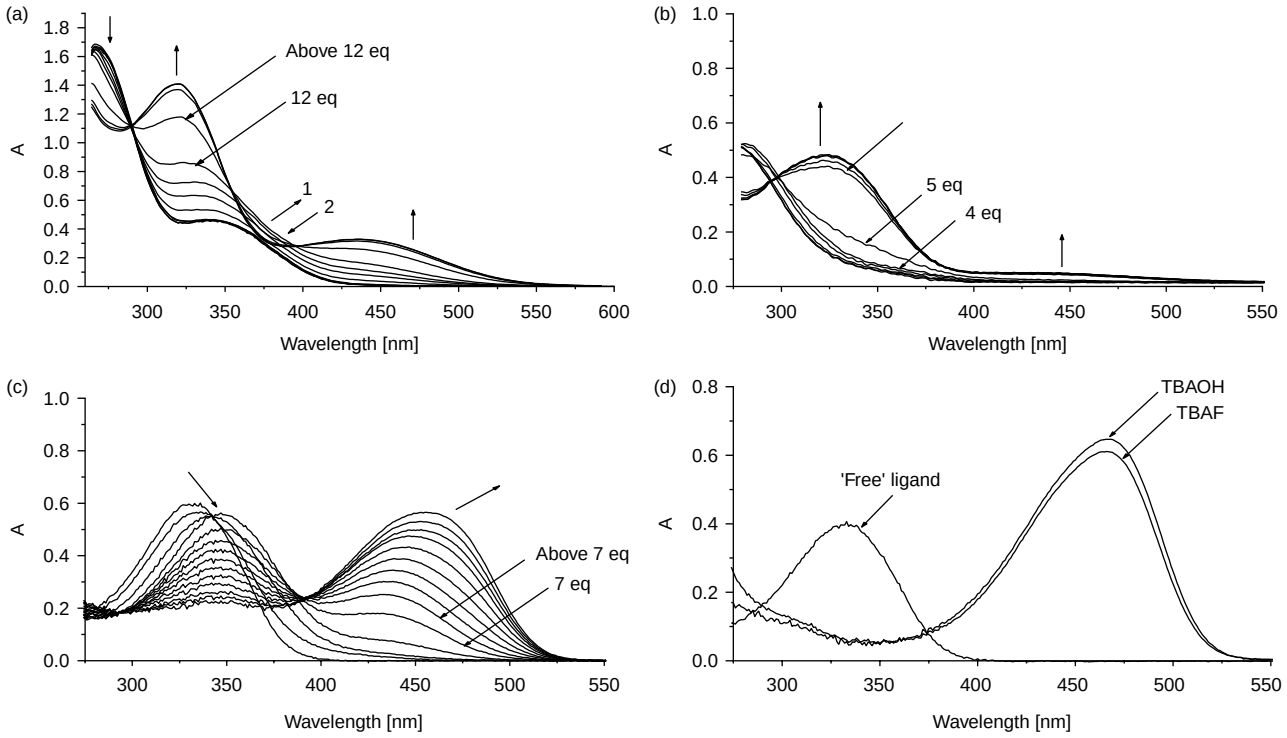

Figure 3. Changes in absorption spectra of ligands **L1**–**L3** upon titration with fluorides (TBAF): (a) **L1** (8.02×10^{-5} M), TBAF ($0–1.30 \times 10^{-3}$ M); (b) **L2** (1.86×10^{-5} M), TBAF ($0–2.01 \times 10^{-4}$ M); (c) **L3** (1.75×10^{-5} M), TBAF ($0–3.24 \times 10^{-3}$ M) and (d) the comparison of changes in the presence of fluorides and hydroxide for **L3** (1.14×10^{-5} M), TBAF (2.66×10^{-3} M) and TBAOH (1.75×10^{-5} M) in DMSO.

presence of fluoride anion, intramolecular hydrogen bonds N—H···N are profitably replaced by a stronger N—H···F intermolecular hydrogen bond. Additionally, due to rigidity and planarity of the 2,6-bis(carbamoyl)pyridine residue, C_{arom}—H protons are able to participate in fluoride binding as C_{arom}—H···F weak hydrogen bonds (cf. *13a–c, 27*). As a consequence, the **L3**·F^- formed complex is fully symmetric. It manifests in pattern of aromatic proton signals in ^{1}H NMR spectrum (see Section 4).

From the NMR titration experiment, the stoichiometry and the stability constant value of the complex formed were estimated using molar ratio (Figure 4(b)) and Scott's method. The molar ratio plot indicates the formation of a 1:1 complex which is satisfactorily confirmed by Scott's

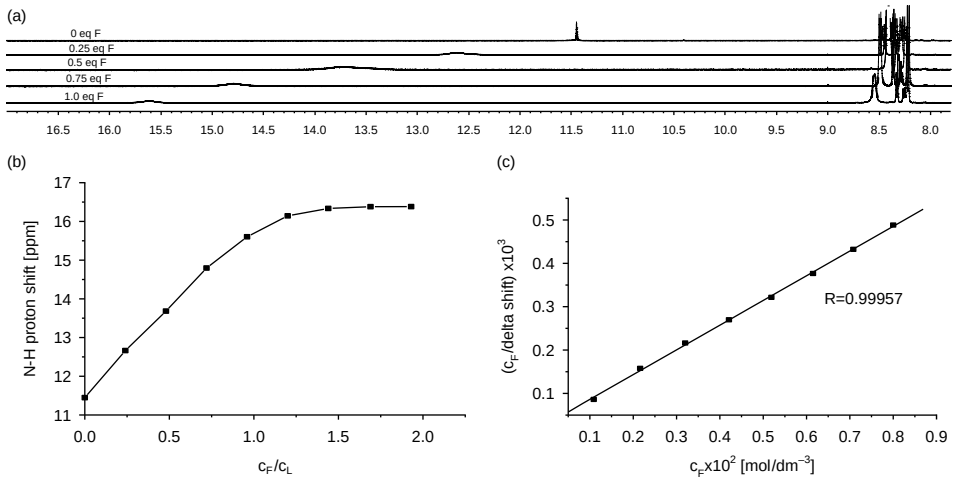

Figure 4. Parts of ^{1}H NMR spectra (8–17 ppm) of **L3** (4.62×10^{-3} M) titration with fluorides in DMSO: (a) changes in the chemical shift of the N—H proton signal; (b) molar ratio plot and (c) Scott's plot.

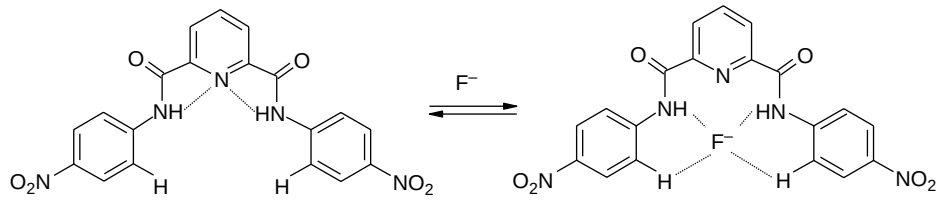

Scheme 1. Proposed mechanism of fluoride binding by **L3**.

linear plot (Figure 4(c)). The stability constant value for the **L3**·F^- complex was estimated from Scott's equation (*31a*) which is a modification of the Benesi–Hildebrand (*31b*) method:

$$\frac{[A]}{\Delta} = \frac{1}{\Delta_0 K} + \frac{[A]}{\Delta_0},$$

where $[A]$ is the molar concentration of anions, Δ is the observed change in chemical shift for a given anion concentration and Δ_0 is the chemical shift change between a complex and the 'free' ligand. The equation was solved by graphical method, where the slope for K and the intercept for Δ_0 are required. For ligand **L3**, the value of stability constant for the 1:1 fluoride complex in DMSO was estimated as $\log K = 3.28$.

Similar experiments carried out in pure DMSO were done for ligands **L1**–**L3** in DMSO–water (95:5, v/v) mixture. In the water-containing system, colour changes were observed only in the case of TBAF and TBAOH (excess, added as solid) with the most evident colour change for ligand **L3**. Under titration conditions, in mixed solvent system, negligible changes were observed in absorption spectra of **L1** and **L2** upon addition of TBAF solution. Better perceptible changes, however less spectacular than in pure DMSO, were found upon **L3** titration with fluorides (data not shown). **L3** in DMSO–water (95:5, v/v) mixture shows absorption maximum at 332 nm. Upon titration, it shifts slightly, resulting in $\lambda_{max} = 344$ nm and a new band of lower intensity appears successively at ~430 nm. One isosbestic point (341 nm) indicates two species under equilibrium and the stoichiometry obtained from the molar ratio plot (data not shown) 1:2 (L:F) suggests ligand deprotonation rather than fluoride complexation under conditions of spectrophotometric titration.

It was expected that ligands having additional hydrogen bond donors (e.g. OH groups; **L4**, **L5**) will influence not only anion–ligand interaction but also spectral changes caused by the presence of electron donor/acceptor residues located in different positions of the molecules. In DMSO, among all the investigated anions, significant spectral and colour changes of **L4** and **L5** solutions were observed in the presence of fluorides, dihydrogen phosphates, acetates and benzoates. To exclude or confirm deprotonation, experiments with TBAOH solution were also carried out. For both ligands **L4** and **L5**, colour changes in the presence of 1 equiv. of TBA salts were almost identical for fluorides, acetates, benzoates and hydroxide. In contrast to **L4**, noticeable, by the naked eye, but less visible changes were found for dihydrogen phosphate in the case of **L5**. Colour changes in the presence of 1 equiv. of the respective TBA salts and TBAOH for ligands **L4** and **L5** are shown in Figure 5(a) and (b). Comparing the above-mentioned ligands **L1**–**L3**, where a relatively large excess of fluoride is needed to observe remarkable colour changes, for **L4** and **L5**, colour changes at equimolar concentrations of ligand and the respective anion were observed. It may be attributed to the presence of phenolic OH groups in the structure of the investigated compounds.

Comparison of the colour changes for ligand **L5** in the presence of TBA salts, i.e. fluorides, acetates and benzoates, and TBAOH suggests that dominating process might be deprotonation. There are four dissociable protons in the studied amides: two phenolic and two from amide groups. In the case of **L4**, colour changes in the presence of TBAOH are not as spectacular (large excess cause orange colour of ligand solution) as for ligand **L5**, where colour changes from pale yellow to orange (at 1 equiv. of fluorides), it is red and purple to navy blue in the extreme case. For both ligands, the colour changes in the presence of TBA salts were associated with the bathochromic shift of absorption bands in UV–vis spectra. The shift is larger for **L5** than for **L4**. Such behaviour is often observed for the ionised chromophore molecules. The difference in colour changes for ligands **L4** and **L5** may be explained, e.g. by the different location of the electron-withdrawing nitro group in relation to OH and NH groups.

Even though visible changes might suggest deprotonation rather than complexation of **L4** and **L5**, UV–vis titration with TBA salts was carried out in DMSO. Changes upon titration with acetate (Figure 6(a)) and dihydrogen phosphate (Figure 6(b)) are exemplified for ligand **L5** (because of more significant spectral changes). Changes upon titration with fluorides and benzoates were similar to those observed for acetates; however, there are most distinctive for fluorides and next for acetates and benzoates. The smallest changes were observed for dihydrogen phosphates. This trend is in agreement with the basicity order of the studied anions:

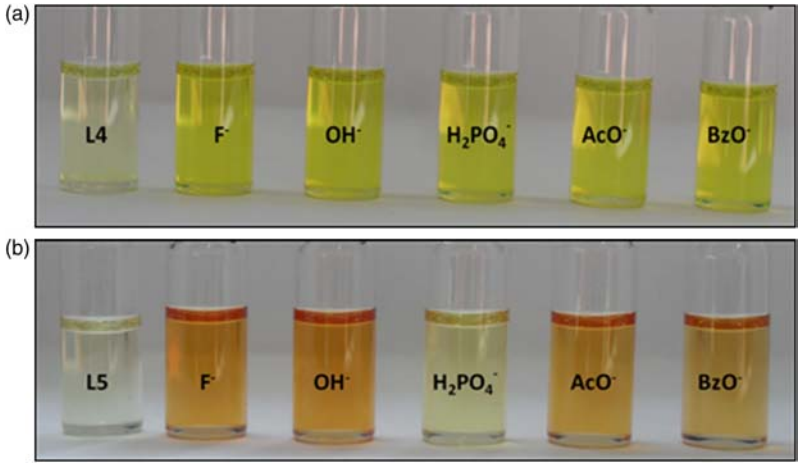

Figure 5. Colour changes of ligands in DMSO: (a) **L4** (1.87×10^{-4} M) and (b) **L5** (2.19×10^{-4} M) solutions in the presence of 1 equiv. of TBA salts.

$F^- > CH_3COO^- > BzO^- > H_2PO_4^-$. Figure 6(c) shows registered limiting spectra and Figure 6(d) shows molar ratio plots for the respective ligand–anion pairs. From molar ratio plots it is evident that the systems equilibrate more or less significantly at different concentrations of the added salts. It seems that under titration conditions the main process is deprotonation of the ligand in the case of fluorides and acetates, whereas for benzoates and dihydrogen phosphates (for 1:1 stoichiometry) binding *via* hydrogen bond formation might be taken into consideration. Stability constant values ($\log K$) for 1:1 complexes calculated with the OPIUM (*32*) program for benzoates and dihydrogen phosphates are 2.83 ± 0.01 and 2.51 ± 0.06, respectively.

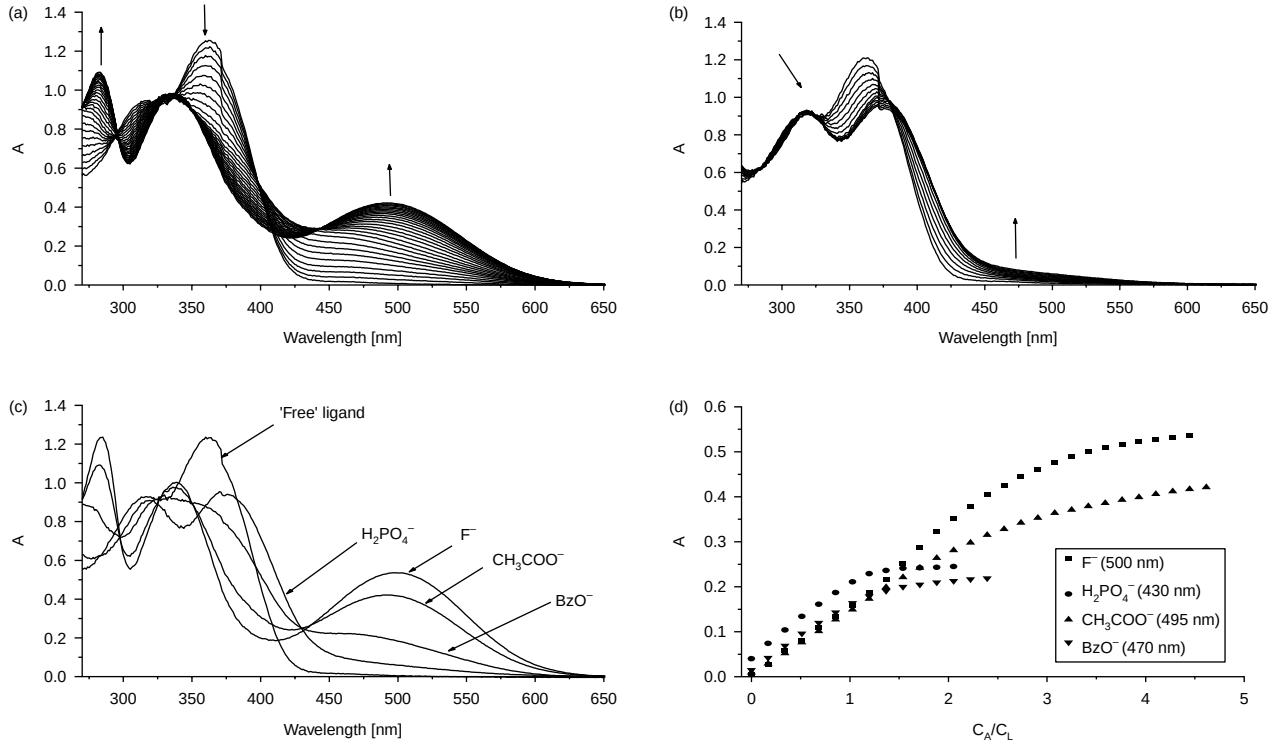

Figure 6. Changes in absorption spectra upon titration of **L5** (4.75×10^{-5} M) with (a) acetates ($0–2.03 \times 10^{-4}$ M); (b) dihydrogen phosphates ($0–9.99 \times 10^{-5}$ M) as TBA salts in DMSO; (c) the limiting spectra obtained during titration of **L5** with fluorides, acetates, dihydrogen phosphates and benzoates and (d) molar ratio plots for the respective anions in DMSO.

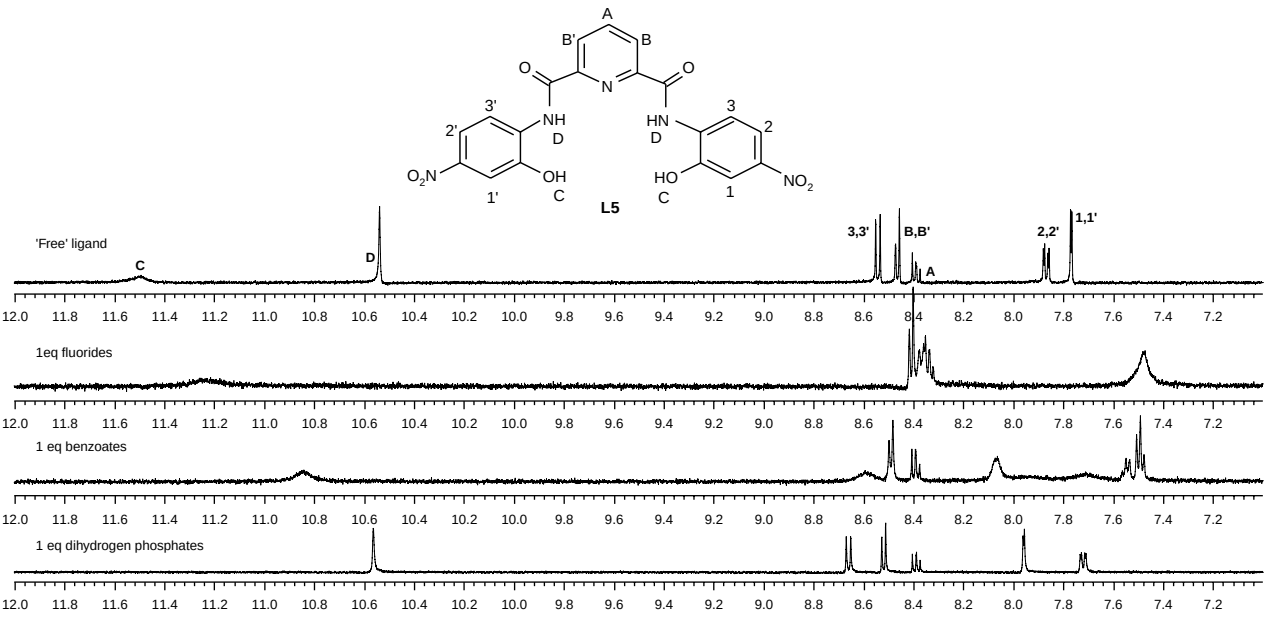

Figure 7. ^{1}H NMR spectra of **L5** (2.60×10^{-3} M) in the presence of 1 equiv. of fluorides, benzoates and dihydrogen phosphates as TBA salts in DMSO-d_6.

To evaluate the possible mechanism of anion–receptor **L5** interaction, ^{1}H NMR (DMSO-d_6) spectra were taken for pure sample and after addition of 1 equiv. of guests (Figure 7).

In the presence of 1 equiv. of the salt protons from the OH residues (C) are not observed, suggesting probable deprotonation. Nevertheless, considering the low intensity of the OH proton signal for the free ligand might be hardly observed in spectra registered in the presence of TBA salts. From downfield shifting of the N—H protons (D) signal in the presence of anions, formation of H-bond might be deducted. The largest shift was observed for fluorides ($\Delta\delta = +0.72$ ppm), then for benzoates ($\Delta\delta = +0.32$ ppm) and acetates ($\Delta\delta = +0.28$ ppm). The smallest shift of N—H signal was observed for dihydrogen phosphate ($\Delta\delta = +0.02$ ppm). Signals of aromatic protons are shifted upfield in the presence of fluorides, acetates (data not shown, see Section 4) and benzoates; however, the nature of these changes is different for benzoates and fluorides. In the presence of fluorides, signals of all aromatic protons are shifted upfield (similarly as in the presence of TBAOH, see Section 4). Protons 1,1′ and 2,2′ are observed as a broad singlet at 7.48 ppm while signal of 3,3′ protons is shifted to 8.41 ppm. For benzoates, more complicated spectrum was obtained, because of additional broad signals of aromatic protons form the anionic form of benzene derivative. Protons 3,3′ of the amidophenolic residue were slightly shifted downfield to 8.48 ppm ($\Delta\delta = -0.06$ ppm), whereas 1,1′and 2,2′ protons are observed as multiplets of integration corresponding to one and three protons at 7.58–7.52 and 7.51–7.46 ppm, respectively. Proton A of pyridine ring was observed as a triplet with the same chemical shift found for free ligand (8.40 ppm). From the changes of chemical shifts for the respective protons, it may be deducted that benzoate protons might be involved in ligand–anion interactions (in a spectrum of pure TBA benzoate aromatic protons are sharp signals at 7.80–7.78 and 7.19–7.18 ppm). Opposite to the anions mentioned above, the chemical shifts alter differently in the case of dihydrogen phosphates. The largest change in chemical shift for aromatic protons is found for protons 1,1′ ($\Delta\delta = +0.19$ ppm) and 3,3′ ($\Delta\delta = +0.12$ ppm). 2,2′ protons are shifted downfield ($\Delta\delta = -0.16$ ppm). It indicates that dihydrogen phosphate anion mainly interacts with **L5** ligand (or its dianion) *via* formation of O—H$\cdots$O$^-$ hydrogen bonds, whereas the N–H protons are involved to a smaller degree compared to small spherical fluorides. The differences may reflect steric effect of the relatively bulky, tetrahedral anion. The proposed models of **L5**–dihydrogen phosphate anion interaction is shown in Scheme 2(a),(b).

Considering colour changes of solution, in the presence of 1 equiv. TBA salts, high selectivity for **L4** and **L5** was not stated in DMSO. Nonetheless, it was found that for **L5** the use of large excess of TBA salts (50-fold) enables visual differentiation among the fluorides, acetates, dihydrogen phosphates and benzoates (see Figure 8). This is in contrast to **L4**, where changes in absorption spectra were also observed in the presence of the mentioned anions; however, no special selectivity towards any of them was found. In all cases, colour changes to intensive yellow which is connected with new absorption maximum formation at

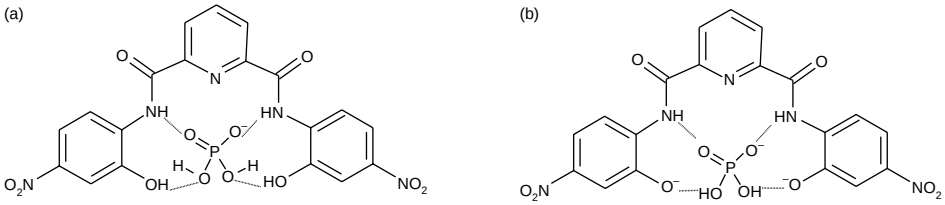

Scheme 2. Proposed models of **L5**–dihydrogen phosphate anion interaction based on hydrogen bonds.

the ~450 nm of different intensity depending on the kind of the added anion salt. Colour and spectral changes for **L4** and **L5** in the presence of 50-fold excess of TBA salts are compared in Figure 8(c),(b). Under such conditions, ligand **L5** may work as a naked-eye anion sensor where the most probable anion recognition mechanism is based on both ligand deprotonation and different types of deprotonated ligand–anion interactions dependent on the type and anion basicity.

To extend the possible application for anion sensing, similar experiments with **L5** were carried out in a mixed, water-containing, solvent system, i.e. DMSO–water (95:5). Colour and spectral changes in this system are shown in Figure 9. In the presence of both 1 and 50 equiv. of TBA salts and TBAOH, selective response towards dihydrogen phosphate was found. Additionally, at higher concentrations of TBA salts, new absorption bands appear allowing differentiation of ligand's response towards hydroxide ($\lambda = 494$ nm), fluorides ($\lambda = 485$ nm), acetates ($\lambda = 480$ nm) and benzoates ($\lambda = 470$ nm) in the water-containing solvent system.

2.3 X-ray studies

Slow evaporation of methanol from the equimolar mixture of **L4** and TBAF resulted in formation of crystals suitable for the X-ray diffraction study. The substance crystallises in triclinic $P\bar{1}$ space group with four $^{n}Bu_4N^+$ cations and two anions present in the unit cell ($Z = 2$).

From the obtained results it is evident that in a solid state, N—H protons, although directed towards the cavity centre, are not engaged in ligand–anion interaction (Figure 10). The molecule of **L4** is not planar and fluoride anion is located above the plane of the molecule. Mean plane defined by the six pyridine atoms forms dihedral angles of 34.13° and 9.89° with pending C1—C6 and C14—C19 hydroxynitrophenyl rings, respectively.

The measured distance O···F 2.8 Å formally corresponds to weak hydrogen bond; however, OH protons are not observed in the Fourier electron density map, which might suggest that one or two OH groups are deprotonated. Charge balance indicates that if a fluoride anion is present then one group is OH and the second is O^-. The presence of HF molecule and phenolate dianion is unlikely because the acidity of HF is higher than the acidity of phenol.

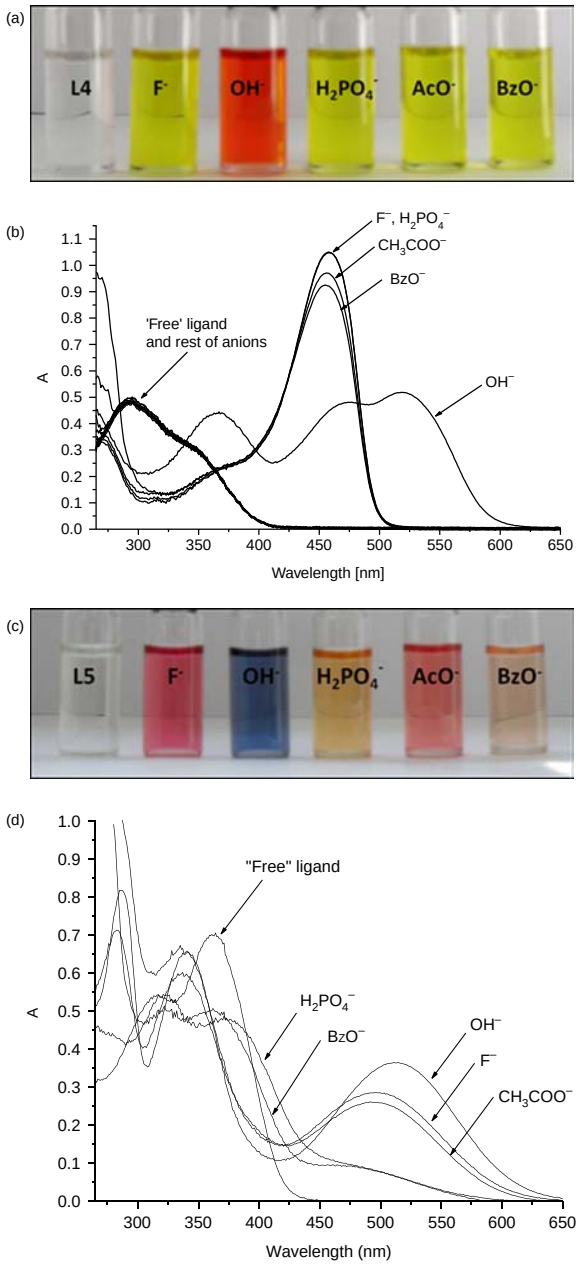

Figure 8. **L4** and **L5** (8.5×10^{-5} M) interactions with anions: (a) and (c) colour changes of ligands' solution; (b) and (d) changes in absorption spectra observed upon addition of 50-fold excess of the respective TBA salts and hydroxide in DMSO (registered in quartz cuvettes of 2 mm path length).

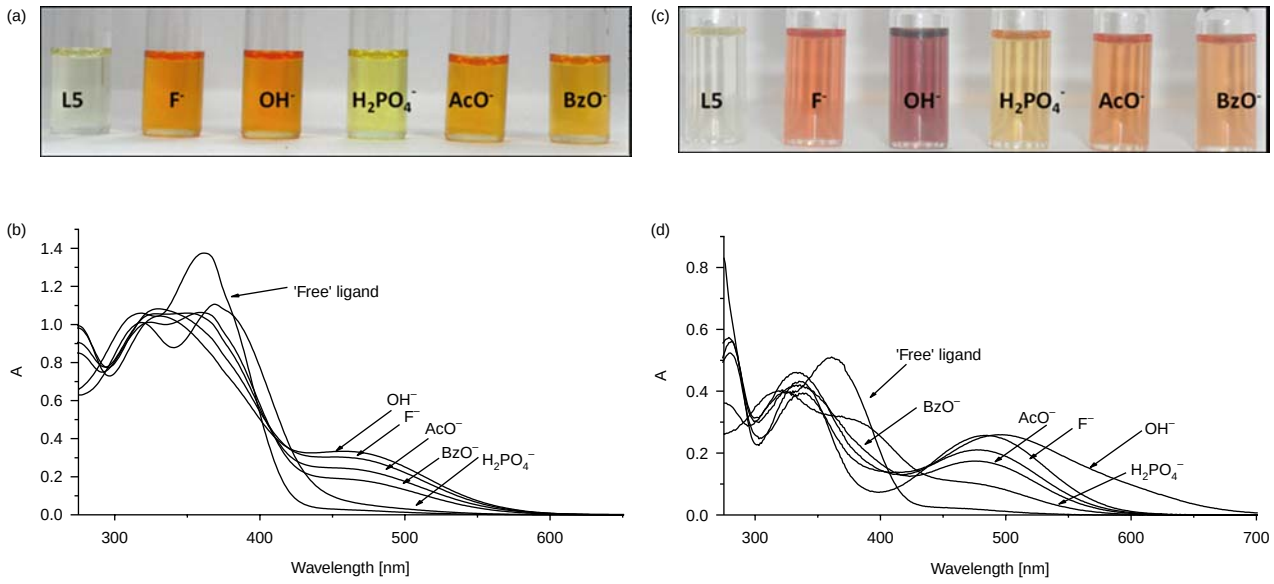

Figure 9. Colour and spectral changes of **L5** in DMSO–water (95:5). (a) and (b) **L5** (2.9×10^{-4} M) in the presence of 1 equiv. of TBA salts; (c) and (d) **L5** (9.9×10^{-5} M) in the presence of 50 equiv. of TBA salts (registered in quartz cuvettes of 2 mm path length).

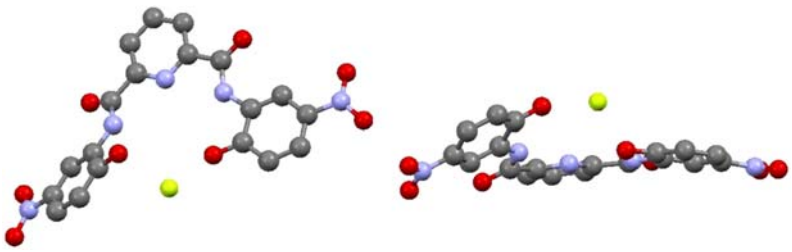

Figure 10. X-ray crystal structure of **L4** crystals formed in the presence of TBAF ($^{n}Bu_4N$ cations and H-atoms are omitted for clarity).

Crystal data and details of structure refinement for **L4**·F^- are presented in Table 1.

3. Conclusions

A simple, high-yielding method for preparation of chromogenic diamides **L1**–**L5** derived from isomeric nitroanilines and aminonitrophenols was presented. For the obtained ligands, studies of anion recognition and its possible nature were carried out in DMSO and its mixture with water. *N*,*N*′-Bis(nitrophenyl)pyridine-2,6-dicarboxamides undergo mainly deprotonation at lower concentrations. However, as shown for **L3**, fluorides are able to interact with this ligand *via* hydrogen bond formation at higher concentration of both the ligand and TBAF. *N*,*N*′-Bis(2-hydroxy-4-nitrophenyl)-pyridine-2,6-dicarboxamide (**L5**) shows dihydrogen phosphate selective response in both DMSO and its mixture with water. It extends possible application of this compound as dihydrogen phosphate receptor. **L5** may also be used at high salt concentration as naked-eye sensor towards selected anions in DMSO and to some extent in the water-containing solvent system. Such selectivity enables preparation of dry tests for rapid anion detection.

4. Experimental

4.1 General procedures and materials

All chemicals were purchased from commercial sources and were used without further purifications. Perchlorate salts (Caution!) should be regarded as potentially explosive and handled with care. Dimethylformamide (DMF) for syntheses was dried over A4 molecular sieves A4. Thin layer chromatography: aluminium sheets covered with $60F_{254}$ were from Merck, Darmstadt, Germany. ^{1}H NMR spectra were recorded at 200 or 500 MHz and ^{13}C NMR at 125 MHz on a Varian instrument. Chemical shifts are reported as δ (ppm) values in relation to tetramethylsilane. FTIR spectra were recorded on a Mattson Genesis II instrument. UV–vis spectra were recorded on an UNICAM UV 300 apparatus in 1.0 cm and 2 mm quartz cells. Mass spectrometry was conducted on an AMD-604 apparatus (EI method, 70 eV) and Mariner (ESI method).

Ion binding studies were performed by UV–vis titration of the ligand solution in DMSO with the respective TBA salt (for anions) or with the perchlorates (for metal cations). The stability constant values were calculated with the use of

Table 1. Crystal data and details of structure refinement for **L4**·F^-.

Empirical formula	$2(C_{16}H_{36}N^+), C_{19}H_{11}N_5O_8^-, F^-$
Formula weight	941.24
Temperature	295(2) K
Wavelength	0.71073 Å
Crystal system	Triclinic
Space group	$P\bar{1}$
Unit cell dimensions	$a = 9.2891(10)$ Å, $\alpha = 99.069(9)°$ $b = 12.4727(15)$ Å, $\beta = 90.159(8)°$ $c = 25.736(3)$ Å, $\gamma = 108.167(10)°$
Volume	2793.44 $Å^3$
Z	2
Density (calculated)	1.119 Mg/m^3
Absorption coefficient	0.078 mm^{-1}
$F(0\,0\,0)$	941.24
Theta range for data collection	2.41–25.10°
Index ranges	$-9 > h > 11$; $-14 > k > 14$; $-30 > l > 26$
Reflections collected	17,492
Independent reflections	9931; 2470 ($I > 2\sigma(i)$)
Completeness to theta = 25.10°	0.999
Refinement method	Full-matrix least squares on F^2
Data/restraints/parameters	9926/416/631
Goodness-of-fit on F^2	0.910
Final R indices [$I > 2$sigma(I)]	$R_1 = 0.0966$, $wR_2 = 0.2323$
R indices (all data)	$R_1 = 0.2983$, $wR_2 = 0.3395$
Largest diff. peak and hole	0.363 and −0.178 e/$Å^3$

the OPIUM (*32*) program on the basis of titration experimental data.

4.2 Synthesis

4.2.1 General procedure for pyridine-2,6-dicarboxylic acid amides

Pyridine-2,6-dicarboxylic acid chloride (1 mmol) was added in portions to a solution of nitroamine or to the respective nitroaminophenol (2 mmol) and triethylamine (2.2 mmol) in DMF (20 ml). The mixture was heated for 12 h at 60°C. The cooled reaction mixture was diluted with water. The solid was filtered off and washed with water, and crystallised from methanol to obtain pure products.

N,*N*′-Bis(2-nitrophenyl)pyridine-2,6-dicarboxamide (**L1**): 89%, yellow solid, $R_f = 0.49$ (methylene chloride); mp 245–246°C; ^{1}H NMR (500 MHz, DMSO, 25°C): $\delta = 7.51$ (2H, t, $J = 8.7$ Hz; Ar-*H*); 7.89 (2H, t, $J = 8.3$ Hz; Ar-*H*); 8.17–8.20 (4H, m; Ar-*H*); 8.37–8.44 (3H, m; Ar-*H*); 11.75 ppm (2H, s; N*H*); ^{13}C NMR (125 MHz, DMSO, 60°C): $\delta = 162.4$; 148.7; 141.5; 135.7; 132.5; 126.6; 126.3; 126.2; 125.3 ppm; FTIR (KBr): $\nu = 649$; 683; 745; 786; 1001; 1069; 1146; 1231; 1238; 1337; 1440; 1501; 1538; 1608; 1698; 3096; 3288; 3361; 3376 cm^{-1}. UV–vis (DMSO): $\lambda_1(\varepsilon_1) = 261$ (2.2×10^4), $\lambda_2(\varepsilon_2) = 345$ (5.9×10^3); HRMS (EI): *m*/*z* calcd for $C_{19}H_{13}N_5O_6$ [M^+]: 407.08658; found 407.08535.

N,*N*′-Bis(3-nitrophenyl)pyridine-2,6-dicarboxamide (**L2**): 83%, pale yellow solid, $R_f = 0.69$ (CH_2Cl_2/acetone 100:1); mp > 305°C; ^{1}H NMR (500 MHz, DMSO-d_6, 25°C): $\delta = 7.78$ (2H, t, $J = 8.1$ Hz; Ar-*H*); 8.07 (2H, dd, $J_1 = 8.3$ Hz $J_2 = 1.5$ Hz; Ar-*H*); 8.35–8.39 (3H, m; Ar-*H*); 8.46 (1H, s; Ar-*H*); 8.48 (1H, s; Ar-*H*); 8.99 (2H, t, $J = 1.9$ Hz; Ar-*H*); 11.37 ppm (2H, s; N*H*); ^{13}C NMR (125 MHz, DMSO-d_6, $t = 60$°C): $\delta = 162.2$; 148.4; 148.2; 140.2; 139.3; 130.2; 126.9; 125.8; 118.8; 114.9 ppm; FTIR (KBr): $\nu = 519$; 597; 665; 736; 817; 880; 1000; 1071; 1150; 1243; 1299; 1348; 1424; 1484; 1259; 1587; 1602; 1677; 3078; 3109; 3312 cm^{-1}; UV–vis (DMSO): $\lambda_{max}(\varepsilon_{max}) = 278$ (3.0×10^4); HRMS (EI): *m*/*z* calcd for $C_{19}H_{13}N_5O_6$ [M^+]: 407.08658; found 407.08459.

N,*N*′-Bis(4-nitrophenyl)pyridine-2,6-dicarboxamide (**L3**): 90%, yellow solid, $R_f = 0.61$ (CH_2Cl_2/acetone 100:1); mp > 305°C; ^{1}H NMR (500 MHz, DMSO-d_6, 25°C): $\delta = 8.26$ (4H, d, $J = 7.7$ Hz; Ar-*H*); 8.35–8.39 (5H, m; Ar-*H*); 8.48 (2H, d, $J = 7.8$ Hz; Ar-*H*); 11.44 ppm (2H, s; N*H*); ^{13}C NMR (125 MHz, DMSO-d_6, $t = 60$°C): $\delta = 162.2$; 148.3; 144.2; 143.2; 140.2; 126.1; 124.7; 120.5 ppm; FTIR (Nujol): $\nu = 502$; 640; 681; 752; 855; 1000; 1112; 1247; 1332; 1409; 1503; 1536; 1598; 1695; 3080; 3114; 3329 cm^{-1}; UV–vis (DMSO): $\lambda_{max}(\varepsilon_{max}) = 333$ (3.3×10^4); HRMS (EI): *m*/*z* calcd for $C_{19}H_{13}N_5O_6$: 407.08658 [M^+]; found: 407.08567.

N,*N*′-Bis(4-nitrophenyl)pyridine-2,6-dicarboxamide aromatic proton signals in the presence of 0.75 equiv. of TBAF, **L3**·F^-: ^{1}H NMR (500 MHz, DMSO-d_6, 25°C): $\delta = 8.21$ (4H, d, $J = 9.1$ Hz); 8.28 (1H, t, $J = 7.3$ Hz); 8.36 (2H, d, $J = 7.8$ Hz) 8.45 (4H, d, $J = 8.5$ Hz); 14.78 ppm (broad s).

N,*N*′-bis(2-hydroxy-5-nitrophenyl)pyridine-2,6-dicarboxamide (**L4**): 67%, grey solid, $R_f = 0.56$ (CH_2Cl_2/metanol 15:2); mp > 305°C; ^{1}H NMR (200 MHz, DMSO-d_6, 25°C): $\delta = 7.13$ (2H, d, $J = 8.9$ Hz; Ar-*H*); 8.02 (2H, dd, $J_1 = 8.9$ Hz, $J_2 = 2.7$ Hz; Ar-*H*); 8.32–8.46 (3H, m; Ar-*H*); 9.09 (2H, d, $J = 2.7$ Hz; Ar-*H*); 10.43 (2H, s; N*H*); ~12 ppm (~1.3H, broad s, O*H*); ^{13}C NMR (125 MHz, DMSO-d_6, $t = 60$°C): $\delta = 161.3$; 154.2; 148.4; 140.5; 139.5; 125.9; 125.5; 121.4; 116.1; 114.8 ppm; FTIR (KBr): $\nu = 641$; 748; 829; 893; 948; 1001; 1077; 1284; 1340; 1440; 1494; 1538; 1595; 1692; 3094; 3125; 3356; 3503 cm^{-1}; UV–vis (DMSO): $\lambda_{max}(\varepsilon_{max}) = 294$ (2.4×10^4); HRMS (ESI negative-ion): *m*/*z* calcd for $C_{19}H_{12}N_5O_8[M-H]^-$: 438.06804; found:438.06695.

N,*N*′-Bis(2-hydroxy-4-nitrophenyl)pyridine-2,6-dicarboxamide (**L5**): 95%, yellow solid, $R_f = 0.67$ (CH_2Cl_2/-metanol 15:2); mp > 305°C; ^{1}H NMR (200 MHz, DMSO-d_6, 25°C): $\delta = 7.77$ (2H, d, $J = 2.4$ Hz; Ar-*H*); 7.86 (2H, dd, $J_1 = 8.9$ Hz, $J_2 = 2.03$ Hz; Ar-*H*); 8.38–8.50 (3H, m; Ar-*H*); 8.54 (2H, d, $J = 8.9$ Hz; Ar-*H*); 10.54 (2H, s; N*H*); ~11.50 ppm (~1.3H, s; O*H*); ^{13}C NMR (125 MHz, DMSO-d_6, $t = 60$°C): $\delta = 161.2$; 148.4; 147.4; 143.3; 140.7; 132.4; 125.8; 119.2; 115.4; 109.2 ppm; FTIR (KBr): $\nu = 744$; 813; 870; 888; 999; 1084; 1118; 1217; 1267; 1339; 1431; 1510; 1534;1595; 1663; 1699; 3093; 3371; 3418 cm^{-1}; $\lambda_1(\varepsilon_1) = 317$ (1.5×10^4), $\lambda_2(\varepsilon_2) = 362$ (2.1×10^4); HRMS (ESI negative-ion): *m*/*z* calcd for $C_{19}H_{12}N_5O_8$ $[M-H]^-$: 438.06804; found: 438.06975.

N,*N*′-Bis(2-hydroxy-4-nitrophenyl)pyridine-2,6-dicarboxamide (**L5**) in the presence of 1 equiv. of TBA acetate: ^{1}H NMR (500 MHz, DMSO-d_6, 25°C): $\delta = 7.55$ (6H, broad distorted d; Ar-*H*); 8.32–8.37 (2H, distorted t; Ar-*H*); 8.40–8.46 (1H, distorted d; Ar-*H*); ~10.82 (broad s; N*H*).

N,*N*′-Bis(2-hydroxy-4-nitrophenyl)pyridine-2,6-dicarboxamide (**L5**) in the presence of 0.75 equiv. TBAOH: ^{1}H NMR (500 MHz, DMSO-d_6, 25°C): $\delta = 6.83$ (1H, distorted s; Ar-*H*); 6.91–6.97 (2H, d; Ar-*H*); 8.18–8.34 (6H, m; Ar-*H*). Proton signals attributed to OH and NH in a free ligand are not observed upon addition of 0.5 equiv. of TBA (at 0.25 equiv., a very weak and broad signal is observed at 10.98 ppm).

4.3 Complexation studies

The stock solutions, for working solution preparation, of the ligands (~10^{-4} M), metal perchlorates and TBA salts (~10^{-2} M) were prepared by weighing the respective quantities and dissolving in volumetric flasks in DMSO (ACS Spectrophotometric Grade, Sigma–Aldrich, Steinheim, Germany). Deionised water (18 MΩ cm, Hydrolab, Poland) was used for the preparation of DMSO–water mixtures. Titrations were carried out in 1 cm path length quartz cuvettes keeping constant volume of the ligand solution (2.3 ml). Titration step was 0.01 ml if not indicated otherwise. The stability constant values were estimated with the use of the OPIUM (*32*) program on the basis of titration data. Absorption spectra of more concentrated ligand solutions were registered in a quartz cuvettes of 2 mm path length.

4.4 X-ray structural analysis of L4 crystal

Crystals of **L4** were obtained by slow methanol evaporation from equimolar mixture of **L4** and TBAF.

X-ray measurements were carried out on a KM4CCD kappa-geometry diffractometer equipped with a Sapphire-2 CCD detector. Enhanced X-ray Mo Kα radiation source with a graphite monochromator was used. Determination of the elemental cell and data collection were carried out at room temperature 295(2) K. The preliminary calculations were made using the CrysAlis software package (Oxford Diffraction, 2008) (*33*). The structure was solved by direct method and refined by full-matrix least-squares procedure based on F^2. Absorption correction was applied in the form of multi-scan procedure. Because of the weak diffraction power of all specimens and poor ratio of observed/collected reflections, all non-hydrogen atoms were refined in isotropic approximation (by ISOR shelx command). Final calculations were carried out using the SHELX-97 program package (*34*). Two terminal atoms C26–C27 and C50–C51 in *n*-butyl chains were refined as disordered over two positions with probabilities 0.668(11)/0.332(11).

5. Supporting Information Available

CIF file for compound **L4** was deposited with the Cambridge Crystallographic Data Centre as supplementary publication number CCDC 857718 (CCDC, 12 Union Road, Cambridge CB2 1EZ, UK; E-mail: deposit@ccdc.cam.ac.uk).

Acknowledgements

E.W.-W. acknowledges support from sources for science in the year 2010–2011, Grant No. N N204 137438. E.W.-W. also thanks Prof. Elżbieta Luboch and Prof. Jan. F. Biernat for the valuable discussion and students Monika Wilamowska and Karolina Hak for their contribution to synthetic work.

References

(1) Conley, D.J.; Paerl, H.W.; Howarth, R.W.; Boesch, D.F.; Seitzinger, S.P.; Havens, K.E.; Lancelot, Ch.; Likens, G.E. *Science* **2009**, *323*, 1014–1015.
(2) Swann, P.F.; Proc, R. *Soc. Med.* **1977**, *70*, 113–115.
(3) (a) Susheela, A.K.; Bhatnagar, M.; Vig, K.; Mondal, N.K. *Fluoride* **2005**, *38*, 98–108. (b) Ding, Y.; Gao, Y.; Sun, H.; Han, H.; Wang, W.; Ji, X.; Liu, X.; Sun, D. *J. Hazard. Mater.* **2011**, *186*, 1942–1946.
(4) (a) Schmidtchen, F.P. *Coord. Chem. Rev.* **2006**, *250*, 2918–2928. (b) Schmidtchen, F.P.; Berger, M. *Chem. Rev.*

1997, *97*, 1609–1646. (c) Beer, P.D.; Gale, P.A. *Angew. Chem. Int. Ed.* **2001**, *40*, 486–516. (d) Gale, P.A. *Coord. Chem. Rev.* **2003**, *240*, 191–221. (e) Suksai, Ch.; Tuntulani, T. *Chem. Soc. Rev.* **2003**, *32*, 192–202. (f) Gunnlaugsson, T.; Glynn, M.; Tocci, G.M.; Kruger, P.E.; Pfeffer, F.M. *Coord. Chem. Rev.* **2006**, *250*, 3094–3117. (g) Gale, P.A. *Acc. Chem. Res.* **2006**, *39*, 465–475. (h) Caltagirone, C.; Gale, P.A. *Chem. Soc. Rev.* **2009**, *38*, 520–563. (i) Gale, P.A.; Garcia–Garrido, S.E.; Garric, J. *Chem. Soc. Rev.* **2008**, 37, 151–190.

(5) Choi, K.; Hamilton, A.D. *Coord. Chem. Rev.* **2003**, *240*, 101–110.

(6) Gale, P.A.; Anzenbacher, Jr., P.; Sessler, J.L. *Coord. Chem. Rev.* **2001**, *222*, 57–102.

(7) Kim, Y.-J.; Kwak, H.; Lee, S.J.; Lee, J.S.; Kwon, H.J.; Nam, S.H.; Lee, K.; Kim, Ch. *Tetrahedron* **2006**, *62*, 9635–9640.

(8) Kondo, S.; Suzuki, T.; Yano, Y. *Tetrahedron Lett.* **2003**, *43*, 7059–7061.

(9) (a) Bondy, Ch.R.; Loeb, S.J. *Coord. Chem. Rev.* **2003**, *240*, 77–99. (b) Kang, S.O.; Begum, R.A.; Bowman-James, K. *Angew. Chem. Int. Ed.* **2006**, *45*, 7882–7894.

(10) (a) Chmielewski, M.J.; Jurczak, J. *Tetrahedron Lett.* **2004**, *45*, 6007–6010. (b) Chmielewski, M.J.; Jurczak, J. *Tetrahedron Lett.* **2005**, *46*, 3085–3088. (c) Chmielewski, M.J.; Jurczak, J. *Chem. Eur. J.* **2005**, *11*, 6080–6094. (d) Chmielewski, M.J.; Jurczak, J. *Chem. Eur. J.* **2006**, *12*, 7652–7667.

(11) Kang, S.O.; Hossain, Md. A.; Bowman-James, K. *Coord. Chem. Rev.* **2006**, *250*, 3038–3052.

(12) Kilah, N.L.; Beer, P.D. Pyridine and Pyridinium-Based Anion Receptors. In *Anion Recognition in Supramolecular Chemistry*; Gale, P.A., Dehaen, W., Eds.; Springer-Verlag: Berlin, Heidelberg, 2010; pp. 301–340.

(13) (a) Winstanley, K.J.; Smith, D.K. *J. Org. Chem.* **2007**, *72*, 2803–2815. (b) Bao, X.; Zhou, Y. *Sens. Actuators B* **2010**, *147*, 434–441. (c) Ju, J.; Park, M.; Suk, J.; Lah, M.S.; Jeong, K.-S. *Chem. Commun.* **2008**, 3546–3548.

(14) (a) Zieliński, T.; Kędziorek, M.; Jurczak, J. *Chem. Eur. J.* **2008**, *14*, 838–846. (b) Dorazco-González, A.; Höpfl, H.; Medrano, F.; Yatsimirsky, A.K. *J. Org. Chem.* **2010**, *75*, 2259–2273. (c) Vega, I.E.D.; Gale, P.A.; Light, M.E.; Loeb, S.J. *Chem. Commun*. **2005**, 4913–4915.

(15) (a) Luecke, H; Quiochio, F.A. *Nature* **1990**, *347*, 402–406. (b) He, J.J.; Quiochio, F.A. *Science* **1991**, *251*, 1479–1481.

(16) Suksai, Ch.; Tuntulani, T. *Top. Curr. Chem.* **2005**, *255*, 163–192.

(17) Martinez-Máñez, R.; Sancenón, F. *Chem. Rev.* **2003**, *103*, 4419–4476.

(18) Fu, T.-M.; Wu, Ch.-Y.; Cheng, Ch.-Ch.; Yang, Ch.-R.; Yen, Y.-P. *Sens. Actuators B* **2010**, *146*, 171–176.

(19) Huang, W.; Lin, H.; Cai, Z.; Lin, H. *Talanta* **2010**, *81*, 967–971.

(20) Zang, Y.-M.; Lin, Q.; Wei, T.-B.; Wang, D.-D.; Yao, H.; Wang, Y.-L. *Sens. Actuators B* **2009**, *137*, 447–455.

(21) Sun, Y.; Wang, G.; Guo, W. *Tetrahedron* **2009**, *65*, 3480–3485.

(22) Moon, K.S.; Singh, N.; Lee, G.W.; Jang, D.O. *Tetrahedron* **2007**, *63*, 9106–9111.

(23) (a) Kavallieratos, R.; de Gala, S.R.; Austin, D.J.; Crabtree, R.H.A. *J. Am. Chem. Soc.* **1997**, *119*, 1545–1546. (b) Kavallieratos, R.; Bertao, C.M.; Crabtree, R.H. *J. Org. Chem.* **1999**, *64*, 1675–1683.

(24) Coles, S.; Frey, J.G.; Gale, P.A.; Hursthouse, M.B.; Light, M.E.; Navakhun, K.; Thomas, G.L. *Chem. Commun.* **2003**, 568–569.

(25) Yamnitz, C.R.; Niegin, S.; Winter, R.K.; Gokel, G.W. *Chem. Commun.* **2010**, 2838–2840.

(26) Carasel, I.A.; Yamnitz, C.R.; Winter, R.K.; Gokel, G.W. *J. Org. Chem.* **2010**, *75*, 8112–8116.

(27) Yin, Z.; Li, Z.; Jiaqi He, W.-Z.; Cheng, J.-P. *Struct. Chem.* **2005**, *16*, 641–647.

(28) Dasgupta, M.; Nag, S.; Das, G.; Nethaji, M.; Bhattacharya, S. *Polyhedron* **2008**, *27*, 139–150.

(29) Perez-Casac, C.; Yatsimirsky, A.K. *J. Org. Chem.* **2008**, *73*, 2275–2284.

(30) (a) Hunter, C.A.; Purvis, D.H. *Angew. Chem.* **1992**, *104*, 779–782. (b) Hunter, C.A.; Purvis, D.H. *Angew. Chem. Int. Ed.* **1992**, *31*, 792–795. (c) Malone, J.F.; Murray, C.M.; Dolan, G.M.; Docherty, R.; Lavery, A.J. *Chem. Mater.* **1997**, *9*, 2983–2989.

(31) (a) Scott, R.L. *Recl. Trav. Chim. Pays-Bas* **1956**, *75*, 787–789. (b) Benesi, H.A.; Hildebrand, J.H. *J. Am. Chem. Soc*. **1949**, *71*, 2703–2707.

(32) Kyvala, M.; Lukeš, I.; Program package "OPIUM" available (free of charge) on http://www.natur.cuni.cz/~kyvala/opium.html.

(33) *Oxford Diffraction CrysAlis CCD and CrysAlis RED*; Version 1.171, Oxford Diffraction Ltd: Abingdon, England, 2008.

(34) Sheldrick, G.M. *Acta Crystallogr. A* **2008**, *64*, 112–122.